Heliyon 9 (2023) e13844

Contents lists available at ScienceDirect

Heliyon

journal homepage: www.cell.com/heliyon

Research article

In vivo modulation of endogenous gene expression via CRISPR/Cas9-mediated 3'UTR editing

Kärt Mätlik [a,1], Soophie Olfat [a,b,1], Mark Cary Cowlishaw [a], Eva Domenech Moreno [c,d], Saara Ollila [d], Jaan-Olle Andressoo [a,b,*,2]

[a] Department of Pharmacology, Faculty of Medicine & Helsinki Institute of Life Science, University of Helsinki, 00290 Helsinki, Finland
[b] Division of Neurogeriatrics, Department of Neurobiology, Care Sciences and Society (NVS), Karolinska Institutet, 17177 Stockholm, Sweden
[c] Helsinki Institute of Life Science, University of Helsinki, 00290 Helsinki, Finland
[d] Translational Cancer Medicine Program, University of Helsinki, 00290 Helsinki, Finland

ARTICLE INFO

Keywords:
3'UTR
GDNF
Gene function
microRNAs
CRISPR/Cas9

ABSTRACT

The 3' untranslated regions (UTRs) modulate gene expression levels by regulating mRNA stability and translation. We previously showed that the replacement of the negative regulatory elements from the 3'UTR of glial cell line-derived neurotrophic factor (GDNF) resulted in increased endogenous GDNF expression while retaining its normal spatiotemporal expression pattern. Here, we have developed a methodology for the generation of *in vivo* hyper- and hypomorphic alleles via 3'UTR targeting using the CRISPR/Cas9 system. We demonstrate that CRISPR/Cas9-mediated excision of a long inhibitory sequence from Gdnf native 3'UTR in mouse zygotes increases the levels of endogenous GDNF with similar phenotypic alterations in embryonic kidney development as we described in GDNF constitutive and conditional hypermorphic mice. Furthermore, we show that CRISPR/Cas9-mediated targeting of 3'UTRs *in vivo* allows the modulation of the expression levels of two other morphogens, *Gdf11* and *Bdnf*. Together, our work demonstrates the power of *in vivo* 3'UTR editing using the CRISPR/Cas9 system to create hyper- and hypomorphic alleles, suggesting wide applicability in studies on gene function and potentially, in gene therapy.

1. Introduction

Emerging data from genome-wide association studies suggest that most disease-associated variants are located in the non-coding regions in the genome, such as in 3'UTRs, indicating that they are likely to affect gene expression levels [1]. To understand how relatively small differences in gene expression levels result in endophenotypes that eventually contribute to differences in disease outcomes, an approach for a relatively fast generation of hyper- and hypomorphic alleles would be useful. Illustrating the importance of gene expression regulation in disease, we recently showed that a relatively small, up to a 2-4-fold difference in endogenous neurotrophic factor GDNF levels can drive a variety of disease-relevant phenotypes, depending on when and where the expression levels are changed, with phenotypes ranging from urogenital tract maldevelopment [2–4] to schizophrenia [5].

Currently, genetic approaches modeling gene expression changes *in vivo* are mostly limited to gene knock-out and transgenic

* Corresponding author. Faculty of Medicine, University of Helsinki, Haartmaninkatu 8, A125, 00290, Helsinki, Finland.
E-mail address: jaan-olle.andressoo@helsinki.fi (J.-O. Andressoo).
[1] Equal contribution.
[2] Lead contact.

https://doi.org/10.1016/j.heliyon.2023.e13844
Received 30 June 2022; Received in revised form 9 February 2023; Accepted 13 February 2023
Available online 24 February 2023

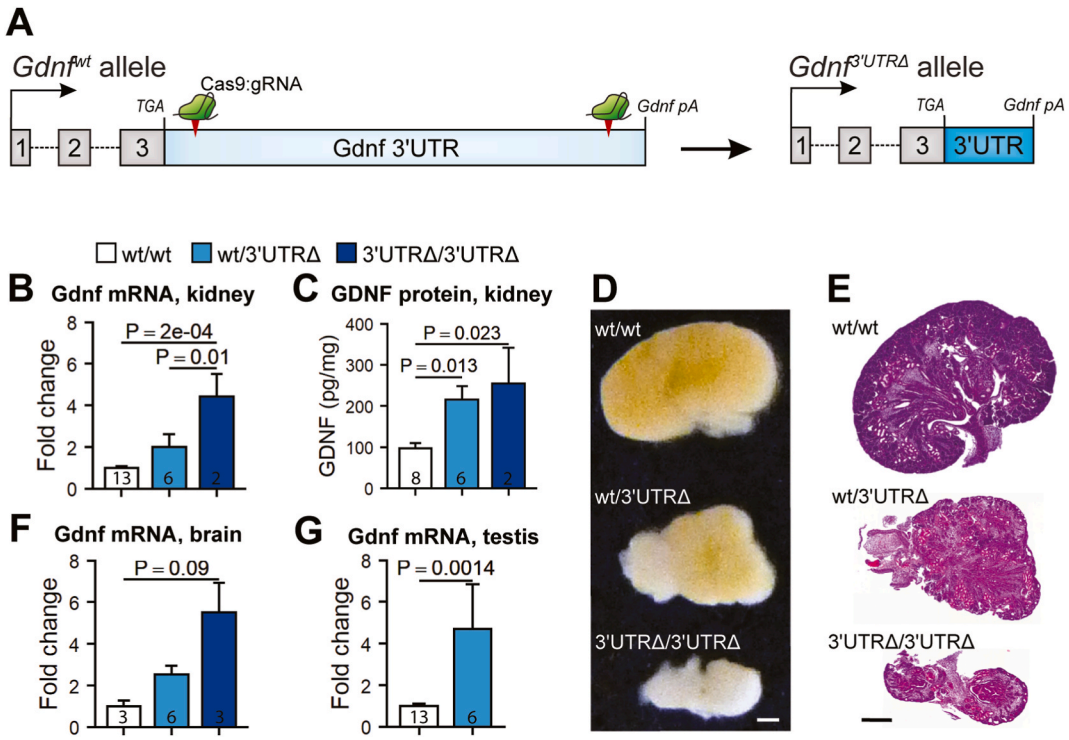

Fig. 1. Gdnf 3'UTR editing with CRISPR/Cas9. **A** Schematic of CRISPR/Cas9-mediated 3'UTR excision with two gRNAs. Stop codon and polyadenylation site of Gdnf mRNA are shown. **B–C** Gdnf mRNA (B) and protein (C) levels in E18.5 kidney after 3'UTR excision. **D-E** Representative images of gross morphology (D) and histology (E) of *Gdnf*$^{3'UTR\Delta}$ mice kidneys at E18.5. **F-G** Gdnf mRNA levels in E18.5 brain (F) and testis (G). Error bars show mean ± SEM. Scale bar, 500 μm.

overexpression, which often results in non-physiological gene expression levels and spatially altered expression patterns. Precise elevation of endogenous gene expression would contribute to our understanding of gene function *in vivo* and open novel gene therapy approaches. Transcriptional gene activation using the CRISPR/Cas9 system is possible but does not limit gene overexpression to naturally transcribing cells. Moreover, the majority of current therapeutic efforts using the CRISPR/Cas9 system focus on gene disruptions [6].

Glial cell line-derived neurotrophic factor (GDNF) is a potent neurotrophic factor [7] and is required for the development of peripheral tissues, such as the kidney [2,8–10]. We recently showed that the replacement of Gdnf 3'UTR with a sequence lacking negative regulation elements increased endogenous Gdnf mRNA and protein levels, while retaining correct GDNF expression pattern [2,5]. Based on our previous observations, we hypothesized that the expression of GDNF and other genes rich with *cis*-regulatory elements, such as microRNA binding sites and AU-rich elements (AREs) in the 3'UTR, could be modulated *in vivo* by targeting their 3'UTR. Here, we use the CRISPR/Cas9 system to excise inhibitory sequences from the genomic regions corresponding to the 3'UTR of *Gdnf* and two additional genes, *Gdf11* and *Bdnf*, in mouse zygotes. We demonstrate that CRISPR/Cas9-mediated 3'UTR shortening can lead to the modulation of endogenous gene expression and associated expected phenotypes *in vivo*. These results represent an efficient method to generate hypermorphic and hypomorphic alleles to study gene function, create disease models, and could open new approaches for CRISPR/Cas9-mediated gene therapy.

2. Results

2.1. Gdnf 3'UTR editing with the CRISPR/Cas9 system

To excise negative regulatory elements from Gdnf 3'UTR, we used the CRISPR/Cas9 system with two gRNAs targeting the beginning and the end of the genomic region corresponding to the 3'UTR, while leaving the translational stop signal and polyadenylation signal intact (Fig. 1A). Based on our previous findings [2,5], we hypothesized that this strategy would result in increased GDNF protein levels. We injected the gRNAs were injected into mouse zygotes and dissected the embryos (designated *Gdnf*$^{3'UTR\Delta}$) at E18.5.

In previous studies, we showed that Gdnf 3'UTR replacement leads to an upregulation of endogenous GDNF levels and early postnatal lethality due to abnormal kidney development [2,3,5]. Specifically, GDNF is required both for the initial step of embryonic kidney development, the outgrowth of the ureteric bud, as well as for ureteric bud branching and bud tip cell migration later in kidney development. Consequently, GDNF knock-out mice die shortly after birth, because they have no kidneys [8–10], whereas mice

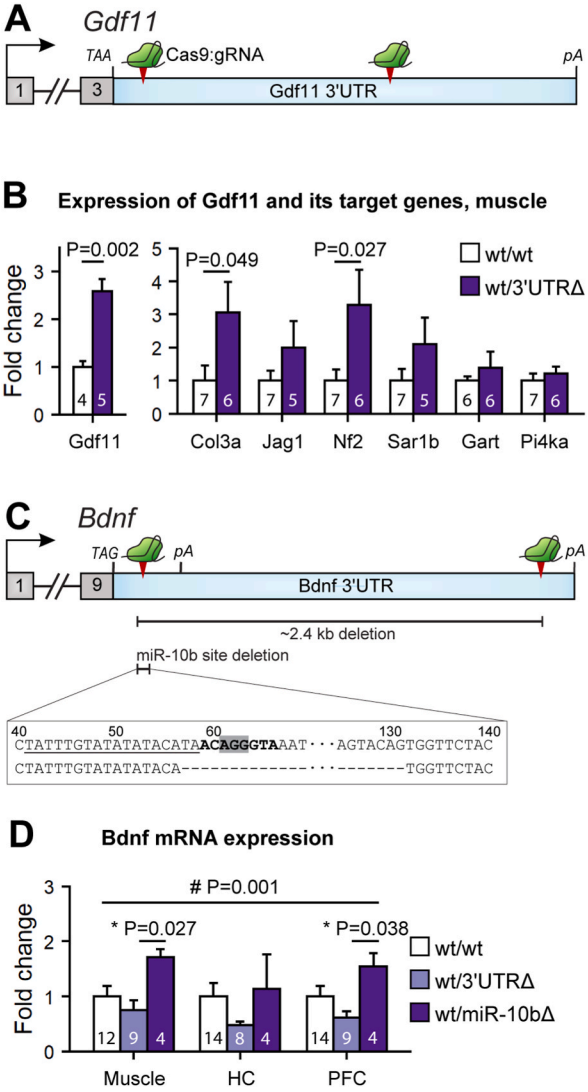

Fig. 2. Validation of 3'UTR shortening approach in *Gdf11* and *Bdnf*. **A** Schematic of Gdf11 3'UTR targeting. Stop codon and polyadenylation site are shown. **B** Expression of Gdf11 (left) and known Gdf11 target genes [14] (right) in E18.5 muscle. **C** Schematic of Bdnf 3'UTR targeting. Stop codon and polyadenylation sites are shown. Deleted nucleotides at the miR-10b site (bold text) are shown in the inset. Shaded nucleotides indicate the protospacer adjacent motif (PAM) site. Underlined sequence denotes gRNA site. **D** Bdnf mRNA expression in P14 tissues after deleting the long (3'UTRΔ) 3'UTR fragment or miR-10b site (miR-10bΔ). *P < 0.05 wt/3'UTRΔ vs wt/miR-10bΔ. #P = 0.001 ANOVA genotype effect between wt/3'UTRΔ and wt/miR-10bΔ across tissues. HC, hippocampus; PFC, prefrontal cortex. Error bars show mean ± SEM.

expressing increased levels of endogenous GDNF exhibit GDNF dose-dependent reduction in kidney size and abnormal kidney histology due to abnormal ureteric bud morphogenesis [2–4]. Therefore, since the importance of GDNF levels to urogenital tract development is well characterized, we analyzed the kidneys of $Gdnf^{3'UTR\Delta}$ embryos to evaluate the phenotypic outcome of CRISPR/Cas9-mediated 3'UTR targeting *in vivo*.

We first measured *Gdnf* expression in the kidneys of $Gdnf^{3'UTR\Delta}$ mice and observed a significant allele-dose-dependent 2-3-fold increase in Gdnf mRNA and GDNF protein levels (Fig. 1B–C). Similar to GDNF hypermorphic ($Gdnf^{hyper}$) and conditional hypermorphic ($Gdnf^{cHyper}$) mice, where we previously observed a similar increase in endogenous GDNF expression [2,3,5], we found that the kidneys of $Gdnf^{wt/3'UTR\Delta}$ and $Gdnf^{3'UTR\Delta/3'UTR\Delta}$ embryos were small and displayed disorganized cortex-medulla structure and cysts in the collecting ducts, compared with wild-type controls (Fig. 1D–E). We then also quantified the expression of Gdnf mRNA in the brain and testis. Similar to $Gdnf^{hyper}$ and $Gdnf^{cHyper}$ mice, the levels of Gdnf transcript were increased by 2-3-fold in $Gdnf^{3'UTR\Delta}$ mice (Fig. 1F–G), indicating that *Gdnf* 3'UTR editing using the CRISPR/Cas9 system in mouse zygotes could be used for fast generation and analysis of *Gdnf* hypermorphic allele *in vivo*.

Table 1
Gdnf and *Bdnf* 3'UTR targeting efficiency and the frequency of individual editing events with each gRNA, determined by genotyping genomic DNA from the tail. Four gRNA combinations (A + C, A + D, B + C, and B + D) were used for each gene, with gRNAs A and B targeting the beginning of the 3'UTR and gRNAs C and D targeting the end of the 3'UTR (see also Figs. 1A and 2C). The values denote the number and percentage of animals of the specified genotype in each group. NA (not applicable) indicates situations where editing events could not have occurred at the specific gRNA sites because the corresponding gRNA was not used (for example, see the editing events at gRNA sites B and D for the A + C combination).

gRNA combination	3'UTR deletion			Individual editing events at gRNA sites				Total
	wt/wt	wt/3'UTRΔ	3'UTRΔ/3'UTRΔ	A	B	C	D	
Gdnf								
A + C	2 (22%)	6 (67%)	0 (0%)	0 (0%)	NA	1 (11%)	NA	9
A + D	6 (100%)	0 (0%)	0 (0%)	0 (0%)	NA	NA	0 (0%)	6
B + C	11 (79%)	3 (21%)	0 (0%)	NA	0 (0%)	0 (0%)	NA	14
B + D	3 (27%)	6 (55%)	1 (9%)	NA	1 (9%)	NA	0 (0%)	11
Total	22 (55%)	15 (37.5%)	1 (2.5%)	0 (0%)	1 (2.5%)	1 (2.5%)	0 (0%)	40
Bdnf								
A + C	2 (25%)	0 (0%)	0 (0%)	6 (75%)	NA	0 (0%)	NA	8
A + D	2 (50%)	1 (25%)	0 (0%)	1 (25%)	NA	NA	0 (0%)	4
B + C	0 (0%)	1 (25%)	0 (0%)	NA	3 (75%)	0 (0%)	NA	4
B + D	10 (100%)	0 (0%)	0 (0%)	NA	0 (0%)	NA	0 (0%)	10
Total	14 (54%)	2 (8%)	0 (0%)	7 (27%)	3 (12%)	0 (0%)	0 (0%)	26

2.2. Validation of the 3'UTR shortening approach to modulate gene expression levels

To investigate if CRISPR/Cas9-mediated 3'UTR shortening could be more broadly applicable to modulate gene expression levels, we targeted the 3'UTRs of two additional morphogens. We selected growth differentiation factor 11 (*Gdf11*, also known as *Bmp11*) and brain-derived neurotrophic factor (*Bdnf*), because these genes have long and conserved 3'UTRs containing microRNA binding sites and/or AREs, and because an ability to regulate the levels of these gene products is believed to hold research and clinical potential in several currently untreatable conditions. For example, ectopic GDF11 application has been shown to restore age-related skeletal and cardiac muscle dysfunction in mice [11], making it an attractive candidate for 3'UTR targeting. BDNF, in turn, is a neurotrophic factor required for synaptic plasticity and learning and memory [12,13].

Similar to Gdnf 3'UTR, we targeted the genomic regions corresponding to Gdf11 and Bdnf 3'UTRs using the CRISPR/Cas9 system (Fig. 2A and **C**). We found that in E18.5 $Gdf11^{wt/3'UTR\Delta}$ embryos, the Gdf11 levels in the skeletal muscle were increased by 2.5-fold (Fig. 2B). To evaluate the downstream consequences of elevated *Gdf11* expression, we next measured the expression of known GDF11 target genes in the skeletal muscle [14]. We found that the expression of several GDF11 targets was significantly increased (Fig. 2B), suggesting that increased *Gdf11* expression in $Gdf11^{wt/3'UTR\Delta}$ embryos resulted in increased GDF11 signaling in the muscle.

We next studied the outcome of 3'UTR deletion on *Bdnf* expression. Bdnf has two alternative 3'UTR isoforms. Of these, the longer isoform has been shown to contain both stabilizing and destabilizing motifs, as well as a dendritic localization element [15–19]. Therefore, we decided to use two approaches for targeting Bdnf 3'UTR (Fig. 2C). First, we deleted a long 3'UTR fragment, by selecting gRNAs targeting the genomic regions corresponding to the beginning and end of the 3'UTR, as described above for *Gdnf* and *Gdf11*. We found that this strategy led to a decreased trend of Bdnf expression in P14 mouse muscle and brain (Fig. 2C–D, 3'UTRΔ), in line with a previous study reporting the presence of mRNA-stabilizing hairpin structure in Bdnf long 3'UTR and a reduction in Bdnf mRNA levels in 'short 3'UTR only' Bdnf 3'UTR knock-in mice [15,19].

Next, building on our previous work showing that BDNF expression is directly regulated by miR-10b binding site in Bdnf 3'UTR [17], we used the CRISPR/Cas9 system with a single gRNA to specifically target miR-10b site in Bdnf 3'UTR (Fig. 2C). Compared to the long 3'UTR excision, deletion of miR-10b motif in Bdnf 3'UTR significantly increased Bdnf levels (Fig. 2C–D, miR-10bΔ). These results suggested that in some cases, identification and targeting of specific 3'UTR regions or *cis*-regulatory elements is necessary to achieve increased gene expression. Overall, our results show that CRISPR/Cas9-mediated 3'UTR shortening can be used to modulate the expression of various genes *in vivo*.

3. Discussion

While gene deletion and transgenic overexpression tools are readily available, our ability to fine-tune endogenous gene expression specifically in natively expressing cells is not well established. Fusion of transcriptional activators to nuclease-dead Cas9 proteins increases transcription from the endogenous locus. However, this method does not limit gene upregulation to endogenously expressing cells. Similarly, BAC/PAC-based transgenes often result in ectopic gene expression. Previous studies have shown that shortening of the 3'UTRs of oncogenes by alternative cleavage and polyadenylation occurs in cancer cells [20] and that CRISPR/Cas9 targeting of 3'UTR elements can be used to modulate endogenous gene expression in vitro [21]. Moreover, recent findings from our laboratory demonstrate that modulating Gdnf 3'UTR *in vivo* through constitutive or conditional 3'UTR replacement increases endogenous GDNF expression, thereby impacting kidney development and brain function [2–5,22,23].

In this study, we addressed the hypothesis that *in vivo* endogenous gene expression can be modulated by CRISPR/Cas9-mediated 3'UTR editing. We show that deleting regulatory regions within the native 3'UTR using the CRISPR/Cas9 system in mouse zygotes leads to the modulation of endogenous gene expression of three different target genes, demonstrating that CRISPR/Cas9-mediated

3'UTR shortening is a feasible approach for both elevating and reducing endogenous gene expression *in vivo*. Our results on *Bdnf* suggest that in cases when the 3'UTR contains putative localization or stabilization elements, endogenous gene upregulation can be achieved by targeting specific negative regulation motifs within the 3'UTR, expanding the number of potential target genes.

Our previous work using genetically modified mice showed that elevating the levels of the neurotrophic factor GDNF in its native expression sites via 3'UTR replacement affects urogenital tract development [2–4] and the function of the adult brain dopamine system [2,5]. We find that the outcomes of endogenous and ectopic GDNF overexpression are often surprisingly different (see Ref. [2] for references). As an example, the mild phenotype of altered dopamine transporter function reported upon conditional deletion of endogenous GDNF in the brain using Nestin-Cre [24,25] could not have predicted that a 2-3-fold elevation in endogenous GDNF using the same Nestin-Cre strain would induce schizophrenia-like phenotypes [5]. These results emphasize that in order to understand how precise regulation of gene expression site and levels controls the development and function of complex tissues such as the brain, it is necessary to develop tools allowing us to modulate gene expression specifically in cells that normally express the gene.

To that end, targeting post-transcriptional regulation while keeping the native promoter and enhancer sequences intact may provide important new information. Moreover, in addition to studies on gene function, increasing endogenous gene expression levels could be used to generate novel disease models, since elevation of endogenous protein levels due to gene duplication, 3'UTR shortening or 3'UTR replacement has been shown to contribute to human diseases including neurodegenerative diseases and cancer [20, 26–28]. Furthermore, given that the development of small molecule compounds is expensive, we propose that modulating target gene expression via the 3'UTR in animal models or human cells could provide a useful analytical step in understanding the consequences of enhancing or reducing a pathway function *in vivo*. Finally, CRISPR/Cas9-mediated 3'UTR targeting could be used as a gene therapy approach, especially for genes that have therapeutic potential but for which ectopic expression is detrimental or even lethal [29,30]. Together, we propose that 3'UTR targeting may help generate better disease models and develop novel therapies for human disease.

3.1. Limitations of the study

The goal of our study was to perform an exploratory, pilot study to address the feasibility of CRISPR/Cas9-mediated 3'UTR targeting to create hypermorphic and hypomorphic alleles. Our study did not analyze protein levels of targeted genes but used established phenotypes such as kidney size and morphology, or known target gene expression as a proxy for estimating the levels of active protein. In addition, we only analyzed animals at late embryonal and early postnatal age to avoid mortality related to predictably severe developmental phenotypes for the kidney (in the case of *Gdnf* [2–5]) and the brain (in the case of *Bdnf* [29]). We note that in specific circumstances where a gene is normally completely repressed via 3'UTR-mediated repression, using the presented method of 3'UTR targeting could theoretically lead to altered expression pattern of an endogenous gene. Potential off-target effects of individual gRNAs were not evaluated. Lastly, we only included three genes in this exploratory study. Therefore, additional studies are necessary to further explore the potential of 3'UTR targeting for *in vivo* gene expression modulation in different tissues and for additional genes.

Author contributions

Conceptualization: K.M., J.-O.A.; Formal analysis: K.M., S.Olfat., M.C.C., E.D.M.; Funding acquisition: J.-O.A.; Investigation: K.M., S.Olfat., Supervision: J.-O.A.; Visualization: K.M., Writing – original draft: K.M., Writing – review & editing: J.-O.A., S.Olfat, S.Ollila.

Declaration of interest

The authors declare that they do not have competing interests.

Data availability

Data and code used for the analysis is available from the corresponding authors upon request.

Acknowledgments

K.M. was supported by the Doctoral Program Brain & Mind and by the Alfred Kordelin Foundation. J.O.A. was supported by the Academy of Finland (grant no. 297727), Sigrid Juselius Foundation, Center of Innovative Medicine (CIMED), Alzheimerfonden, Hjärnfonden, Swedish Research Council (grant no. 2019-01578), Helsinki Institute of Life Science, and by European Research Council (ERC, grant no. 724922).

Appendix

Materials and Methods

Animals. All animal experiments were conducted according to the 3R principles of the European Union Directive 2010/63/EU governing the care and use of experimental animals and following local laws and regulations (Finnish Act on the Protection of Animals Used for Scientific or Educational Purposes (497/2013), Government Decree on the Protection of Animals Used for Scientific or

Educational Purposes (564/2013)). The protocols were authorized by the national Animal Experiment Board of Finland (license numbers ESAVI/11198/04.July 10, 2014 and ESAVI/12046/04.July 10, 2017).

gRNA design and production. Guide RNAs (gRNAs) were designed using the CRISPR Design Tool (crispr.mit.edu) and produced using overlap PCR as in Ref. [31]. The gRNA template was transcribed in vitro with the Megashortscript T7 Kit (cat. no. AM1354, Life Technologies) according to the protocol provided by the manufacturer. An amount of 165 ng of the template was incubated for 5 h at 37 °C. In vitro transcribed RNA was purified with Megaclear Kit (cat. no. AM1908, Life Technologies) according to the manufacturer's recommendations. gRNA integrity was measured with Agilent 2100 Bioanalyzer (Agilent Technologies). To reduce the possibility that one or both of the gRNAs would be inefficient in mediating cleavage by Cas9, we designed two gRNAs to target both the beginning (A, B) and the end (C, D) of the 3'UTR. The following gRNA sequences were used: Gdnf-gRNA-A, CCTGCTACAGTGCGAAGAAA; Gdnf-gRNA-B, CAGTGCGAAGAAAGGGACCA; Gdnf-gRNA-C, CATCTCGAGCAGGTTCGAAT; Gdnf-gRNA-D, CAGCAGGGTAAAGTTTGCGA; Bdnf-gRNA-A, TATTTGTATATATACATAAC; Bdnf-gRNA-B, ATGAAGTTTATACAGTACAG; Bdnf-gRNA-C, ACATCATAGCTACATGTTGG; Bdnf-gRNA-D, TTCTTCGTTTCTGTTCGTTC; Gdf11-gRNA-A, GTATTGCACACTGCTTGGTC; Gdf11-gRNA-B, GTGAGAGGCTTGGTATAGTT; Gdf11-gRNA-C, GCCAGTCCACACAGGTAGTG; Gdf11-gRNA-D, GCCTGATGGCCTTTTTGCAA.

Zygote microinjection. Cas9 mRNA (5meC, Ψ, cat. no. L-6125, Trilink Biotechnologies) and purified gRNAs were injected into the pronucleus at concentrations of 25 ng/ml and 12.5 ng/ml, respectively, in injection buffer containing 0.25 mM EDTA, 10 mM Tris-HCl, pH 7.4. Prior to microinjection, the mixture was centrifuged at 13,200 rpm for 30 min at 4 °C in a standard tabletop centrifuge and the supernatant was collected into a fresh RNase-free tube. Microinjection and embryo transfer were performed at Turku Center for Disease Modeling (*Gdnf*, *Bdnf*) or by Cyagen Biosciences (*Gdf11*), using routine methods. Mouse zygotes were microinjected at one-cell stage with purified gRNAs and *S. pyogenes* Cas9 mRNA. In experiments targeting *Gdnf* and *Gdf11* 3'UTR, survival rate was not evaluated because animals were dissected at embryonic or early postnatal ages. Mice carrying deletions in *Bdnf* 3'UTR were viable and fertile and did not exhibit gross anatomical or behavioral phenotypes.

Genotyping and targeting efficiency. Genomic DNA was isolated from the tail using Extracta DNA Prep for PCR - tissue (cat. no. 95091, Quanta Biosciences, USA). Genotyping was performed using AccuStart II GelTrack PCR SuperMix (cat. no. 95136, Quanta Biosciences, USA) (tail), or with real-time quantitative PCR (qPCR). The following primers were used: Gdnf-F1, GTGAATCGGCCGAGACAATG; Gdnf-F2, AGATGTCGTTCCAGACCCTCT; Gdnf-R, TAACACAAACGACCGAGACATCA, Bdnf-F, AAGGCACTGGAACTCGCAAT; Bdnf-R1, TTGTGCGCAAATGACTGTTTC; Bdnf-R2, AGAGAACAAGGCCACAGACAT. Gdf11-F, TCCCCATTCCTCAAGCCCTA, Gdf11-R1, GCTACTGGAAGGAGAGAGGGA; Gdf11-R2, CCCAAAACTCAGAGCACCCT. PCR products were analyzed on a 2% agarose gel in borate buffer. The efficiency of *Gdnf* and *Bdnf* 3'UTR targeting based on genotyping the tail of F0 animals and the number of individual editing events of each of the used gRNA (determined by sequencing) are shown in Table 1. Note that we observed considerable differences in the efficiencies of individual gRNAs that were not predicted by bioinformatics tools. Since the CRISPR/Cas9 system can result in mosaicism, and because all the genes included in this study have highly specific expression patterns, the genotypes of the F0 animals (in the case of *Gdnf* and *Gdf11* 3'UTR targeting) were further determined from cDNA synthesized from mRNA expressed in each of the analyzed tissues. We reasoned that 3'UTR targeting can affect *Gdnf* expression levels and potential resulting phenotypes only if it occurred in *Gdnf*-expressing cells. Indeed, we found that genotypes occasionally differed between different tissues of the same animal, suggesting that Cas9-mediated DNA cleavage and DNA repair by non-homologous end joining had occurred after the first zygote division. Therefore, we used genotypes identified based on cDNA genotyping in each individual tissue for downstream analyses. In the case of Bdnf, F1 and F2 offspring were genotyped using routine methods.

Isolation of tissues. Pregnant females were deeply anesthetized with CO_2, followed by cervical dislocation and decapitation. $Gdnf^{3'UTR\Delta}$ and $Gdf11^{3'UTR\Delta}$ embryos were dissected at E18.5. $Bdnf^{3'UTR\Delta}$ pups were dissected at P14, by decapitation. Tissues isolated for mRNA and protein analysis were snap frozen and stored at −80 °C until processed for analysis. Samples for histological analysis were immediately fixed in fresh 4% formaldehyde and paraffinized following a standard protocol. The sex of the pups was not determined.

Analysis of mRNA levels. RNA was isolated using RNAqueous Micro Kit (cat. no. AM1931, Thermo Fisher Scientific) according to the protocol provided by the manufacturer. cDNA was synthesized from 150 to 500 ng of total DNase-treated RNA using RevertAid Reverse Transcriptase (cat. no. EP0441, Thermo Fisher Scientific) according to the manufacturer's recommendations. qPCR was performed on a LightCycler 480 instrument using SYBR Green I Master (cat. no. 04887352001, Roche Diagnostics). Each qPCR reaction contained 250 pmol of primers and cDNA corresponding to 0.25 ng of RNA. For normalization, we used β-actin or a combination of β-actin, Hprt (Hypoxanthine Phosphoribosyltransferase 1), Pgk1 (Phosphoglycerate Kinase 1), and Gapdh (Glyceraldehyde 3-phosphate dehydrogenase). qPCR reactions were performed in duplicate. The following primers were used: Actb-F, CTAAGGCCAACCGTGAAAAG; Actb-R, ACCAGAGGCATACAGGGACA; Gdnf-F, CGCTGACCAGTGACTCCAATATGC; Gdnf-R, TGCCGCTTGTTTATCTGGTGACC; Gapdh-F, GCCTCGTCCCGTAGACAAAA; Gapdh-R, ATGAAGGGGTCGTTGATGGC; Hprt1-F, CAGTCCCAGCGTCGTGATTA; Hprt1-R, TGGCCTCCCATCTCCTTCAT; Pgk1-F, TTGGACAAGCTGGACGTGAA; Pgk1-R, AACGGACTTGGCTCCATTGT. Intron-spanning primers were used when possible. Negative control (minus-reverse-transcription or water) was included in each run. The quantification cycle (Cq) values were calculated with LightCycler 480 Software Release 1.5.0 SP1 using the Absolute Quantification/2nd Derivative Max option. Results for a biological repeat were discarded when the Cq value for one or more of the replicates was 40 or 0, when the Cq difference between replicates was >1, or when the standard deviation between technical replicates was >1.

Analysis of protein levels. GDNF protein levels were analyzed using the GDNF Emax Immunoassay System (cat. no. G7620, Promega) according to the manufacturer's protocol. Tissue samples were homogenized in lysis buffer prepared according to the producer's recommendations. The tissue homogenate was centrifuged at 5000 rpm for 15 min at 4 °C and the supernatant was used immediately or stored at −80 °C. The samples were treated with HCl for 15 min and neutralized with NaOH. An amount of 20 µl of the

lysate was loaded onto the multiwell plate. All samples were analyzed in duplicate. GDNF levels were normalized to total protein concentration, measured using DC Protein Assay (cat. no. 5000111, Bio-Rad).

Histological analysis. Dissected tissues were immediately immersed in 4% formaldehyde and paraffinized. For histological analysis, 5-μm paraffin sections were stained with Harris's hematoxylin (Merck) and eosin Y (Sigma-Aldrich). RNA in situ hybridization was performed as previously described [2]. Briefly, fresh 5-μm paraffin sections from embryonic kidney or adult brain were hybridized with RNAscope probes [32] (Advanced Cell Diagnostics) detecting Gdnf mRNA, according to the manufacturer's recommendations. Sections were scanned with a Pannoramic 250 digital slide scanner (3D Histech).

Microarray data analysis. Microarray data from GSE67326 [14] was analyzed from the raw CEL files using the R packages: "affy" to load the files and "limma" for differential gene expression analysis. The model design used in limma was ~0 + group, where the group was in the form "treatment_concentration_time". The GDF11 target gene list was created by taking only into account genes that were significantly expressed (absolute log2-fold-change >0.75 and p-adjusted <0.05) in all the comparisons of GDF11-treated samples against their respective control.

Quantification and statistical analysis

Sample size. Sample size was determined based on previous experience with the analysis of mRNA expression levels. No statistical methods were used to predetermine the sample size.

Rules for stopping data collection. Rules for stopping data collection were not defined.

Data inclusion/exclusion criteria and handling of outliers. Data was excluded based on insufficient quality (assessed immediately after acquisition and before analysis). Quality control parameters, where relevant, are detailed in the corresponding Methods sections above. Grubbs test for outliers was performed when outliers were suspected, and significant outliers ($p < 0.05$) were excluded from downstream analysis.

Research subjects or units of investigation. Research subjects correspond to individual animals. Because of a small number of Bdnf miR-10bΔ mice, their Bdnf mRNA levels were quantified twice (in two qPCR runs) and the replicates were pooled for statistical analysis.

Randomization. Because the animal's genotype determined the experimental group, randomization to treatment was not possible. To reduce possible bias due to environmental variables, only litters including animals from different genotypes were included. Tissue isolation was always performed in random order.

Blinding. The samples were processed before genotyping by investigators blinded to experimental groups.

Statistical analysis. All values are presented as mean ± standard error of the mean. Statistical analysis of the qPCR results was performed as in Ref. [17], using the geometric mean of reference genes for normalization, when appropriate. Plots were prepared with R, using ggplot2 [33]. Statistical significance was calculated using an unpaired Student's *t*-test with two-tailed distribution or one-way analysis of variance (ANOVA), followed by Tukey's *post hoc* test. The level of significance was set at $P < 0.05$.

References

[1] L.A. Hindorff, et al., Potential etiologic and functional implications of genome-wide association loci for human diseases and traits, Proc. Natl. Acad. Sci. U. S. A. 106 (23) (2009) 9362–9367.
[2] A. Kumar, et al., GDNF overexpression from the native locus reveals its role in the nigrostriatal dopaminergic system function, PLoS Genet. 11 (12) (2015) e1005710.
[3] H. Li, et al., Development of the urogenital system is regulated via the 3'UTR of GDNF, Sci. Rep. 9 (1) (2019) 5302.
[4] H. Li, et al., Postnatal prolongation of mammalian nephrogenesis by excess fetal GDNF, Development 148 (10) (2021).
[5] K. Mätlik, et al., Elevated endogenous GDNF induces altered dopamine signalling in mice and correlates with clinical severity in schizophrenia, Mol. Psychiatr. 27 (8) (2022) 3247–3261.
[6] I. Dasgupta, T.R. Flotte, A.M. Keeler, CRISPR/Cas-Dependent and nuclease-free in vivo therapeutic gene editing, Hum. Gene Ther. 32 (5–6) (2021) 275–293.
[7] L.F. Lin, et al., GDNF: a glial cell line-derived neurotrophic factor for midbrain dopaminergic neurons, Science 260 (5111) (1993) 1130–1132.
[8] M.W. Moore, et al., Renal and neuronal abnormalities in mice lacking GDNF, Nature 382 (6586) (1996) 76–79.
[9] J.G. Pichel, et al., Defects in enteric innervation and kidney development in mice lacking GDNF, Nature 382 (6586) (1996) 73–76.
[10] M.P. Sanchez, et al., Renal agenesis and the absence of enteric neurons in mice lacking GDNF, Nature 382 (6586) (1996) 70–73.
[11] Y. Zhang, et al., Role of growth differentiation factor 11 in development, physiology and disease, Oncotarget 8 (46) (2017) 81604–81616.
[12] M. Miranda, et al., Brain-derived neurotrophic factor: a key molecule for memory in the healthy and the pathological brain, Front. Cell. Neurosci. 13 (2019) 363.
[13] A.H. Nagahara, M.H. Tuszynski, Potential therapeutic uses of BDNF in neurological and psychiatric disorders, Nat. Rev. Drug Discov. 10 (3) (2011) 209–219.
[14] M.A. Egerman, et al., GDF11 increases with age and inhibits skeletal muscle regeneration, Cell Metabol. 22 (1) (2015) 164–174.
[15] J.J. An, et al., Distinct role of long 3' UTR BDNF mRNA in spine morphology and synaptic plasticity in hippocampal neurons, Cell 134 (1) (2008) 175–187.
[16] C. Andreassi, A. Riccio, To localize or not to localize: mRNA fate is in 3'UTR ends, Trends Cell Biol. 19 (9) (2009) 465–474.
[17] K. Varendi, et al., miR-1, miR-10b, miR-155, and miR-191 are novel regulators of BDNF, Cell. Mol. Life Sci. 71 (22) (2014) 4443–4456.
[18] K. Varendi, K. Matlik, J.O. Andressoo, From microRNA target validation to therapy: lessons learned from studies on BDNF, Cell. Mol. Life Sci. 72 (9) (2015) 1779–1794.
[19] G.Y. Liao, et al., Dendritically targeted Bdnf mRNA is essential for energy balance and response to leptin, Nat. Med. 18 (4) (2012) 564–571.
[20] C. Mayr, D.P. Bartel, Widespread shortening of 3'UTRs by alternative cleavage and polyadenylation activates oncogenes in cancer cells, Cell 138 (4) (2009) 673–684.
[21] W. Zhao, et al., CRISPR-Cas9-mediated functional dissection of 3'-UTRs, Nucleic Acids Res. 45 (18) (2017) 10800–10810.
[22] K. Matlik, et al., Two-fold elevation of endogenous GDNF levels in mice improves motor coordination without causing side-effects, Sci. Rep. 8 (1) (2018), 11861.
[23] P. Marshall, et al., Elevated expression of endogenous glial cell line-derived neurotrophic factor impairs spatial memory performance and raises inhibitory tone in the hippocampus, Eur. J. Neurosci. 53 (8) (2021) 2469–2482.

[24] J. Kopra, et al., GDNF is not required for catecholaminergic neuron survival in vivo, Nat. Neurosci. 18 (3) (2015) 319–322.
[25] J.J. Kopra, et al., Dampened amphetamine-stimulated behavior and altered dopamine transporter function in the absence of brain GDNF, J. Neurosci. 37 (6) (2017) 1581–1590.
[26] P. Ibanez, et al., Causal relation between alpha-synuclein gene duplication and familial Parkinson's disease, Lancet 364 (9440) (2004) 1169–1171.
[27] M.C. Chartier-Harlin, et al., Alpha-synuclein locus duplication as a cause of familial Parkinson's disease, Lancet 364 (9440) (2004) 1167–1169.
[28] A. Rovelet-Lecrux, et al., APP locus duplication causes autosomal dominant early-onset Alzheimer disease with cerebral amyloid angiopathy, Nat. Genet. 38 (1) (2006) 24–26.
[29] S. Alcantara, et al., BDNF-modulated spatial organization of Cajal-Retzius and GABAergic neurons in the marginal zone plays a role in the development of cortical organization, Cerebr. Cortex 16 (4) (2006) 487–499.
[30] C. Cunha, et al., Brain-derived neurotrophic factor (BDNF) overexpression in the forebrain results in learning and memory impairments, Neurobiol. Dis. 33 (3) (2009) 358–368.
[31] A.R. Bassett, et al., Highly efficient targeted mutagenesis of Drosophila with the CRISPR/Cas9 system, Cell Rep. 4 (1) (2013) 220–228.
[32] F. Wang, et al., RNAscope: a novel in situ RNA analysis platform for formalin-fixed, paraffin-embedded tissues, J. Mol. Diagn. 14 (1) (2012) 22–29.
[33] H. Wickham, ggplot2: Elegant Graphics for Data Analysis, Springer-Verlag, New York, 2016.